

Timing of fungal spore release dictates survival during atmospheric transport

Daniele Lagomarsino Oneto ^{*}, Jacob Golan [†], Andrea Mazzino [‡], Anne Pringle [†], Agnese Seminara ^{*}

^{*}CNRS and Université Côte d'Azur, Institut de Physique de Nice UMR7010, parc Valrose 06108 Nice, France, [†]Departments of Botany and Bacteriology, University of Wisconsin-Madison, Madison, WI, USA, and [‡]Department of Civil, Chemical, and Environmental Engineering, University of Genova and INFN, via Montallegro 1, 16145 Genova, Italy

Submitted to Proceedings of the National Academy of Sciences of the United States of America

The fungi disperse spores to move across landscapes and spore liberation takes different patterns. While many species release spores intermittently, others release spores at specific times of day or night according to intrinsic rhythms. Despite intriguing evidence of diurnal rhythms, why the timing of spore liberation would matter to a fungus remains an open question. Here we use state-of-the-art numerical simulations of atmospheric transport with meteorological data to follow the trajectory of many spores released in the open atmosphere at different times of day, during different seasons and at different locations across North America. While individual spores follow unpredictable trajectories due to turbulence, in the aggregate patterns emerge: statistically, spores released during the day fly for several days, while spores released at night return to the ground within a few hours. Differences are caused by intense turbulence during the day and weak turbulence at night. The pattern is widespread but its reliability varies, for example, day/night patterns are stronger in southern regions, where temperatures are warmer. Results provide a set of testable hypotheses explaining intermittent and regular patterns of spore release as strategies to maximize spore survival in the air. Species with short lived spores reproducing where there is strong and regular turbulence during the day, for example in Mexico, will maximize survival by routinely releasing spores at night. Where cycles are weak, for example in Canada during spring, there will be no benefit to releasing spores at the same time every day. We also challenge the perception of atmospheric dispersal as risky, wasteful, and beyond control of a sporocarp; our data suggest the timing of spore liberation may be finely tuned by a fungus to maximize fitness during atmospheric transport.

A careful reading of the natural history of fungal spore liberation reveals nontrivial patterns. Spores may be released at specific times of the day according to an internal clock, or may be released according to fluctuations in the environment. Some species display regular, nearly circadian rhythms, e.g. the asexual spores of the powdery mildew Genus species are mostly released at midday ([1] and references therein). Other species release spores preferentially at night or early morning, including the plant pathogens *Mycosphaerella fijiensis* (causing wheat leaf blotch and black leaf streak in bananas) [2, 3, 4, 5], *Giberella zeae* (causing crown rot in cereals) [6, 7], *Venturia inaequalis* (the apple scab) [8, 9] as well as several tropical species [10, 11]. Or patterns may be more complex, e.g. the causal agent of blackleg, *Leptosphaeria maculans*, seems to follow different diurnal rhythms in different regions and seasons, with most spores liberated in the morning in England [12] or at night in Canada [13], or early afternoon in Western Australia [14]. Alternatively, there may be no regular pattern, e.g. in different studies of *L. maculans* in Western Australia spores were released intermittently, regardless of location or month [15, 16].

Many authors have attempted to connect the diversity of spore liberation patterns to specific environmental conditions by drawing correlations with local temperature, humidity and wind speed (reviewed in [1, 17, 18]). For example, asexual spores of *Helminthosporium maydis* (syn. = *Bipolaris maydis*) and *Alternaria spp.* are detached from the substrate by intense wind gusts (e.g. [19, 20]). Despite a wealth of data

describing different diurnal or nocturnal patterns of spore liberation, and a nascent understanding of their importance for spore survival [21, 22, 23] the causes of these patterns remain obscure [14, 17].

Atmospheric dispersal is assumed to be both common and dangerous. Cellular material makes up about 25% of the atmospheric particulate and 3% to 11% by weight [24, 25], with crucial implications for health, agriculture and climate. But of the estimated $\sim 10^{21}$ cells riding the atmosphere annually, only a small fraction may survive the journey. Exposure to UV light damage, and to uncontrolled fluctuations in temperature and humidity are the main threats that limit the lifespan of spores in the open atmosphere [26].

To date research has focused on the reach of a spore, in other words, biologists have sought to understand how far a spore will move before deposition, and paid attention to distances traveled. For example, it is generally recognized that spores and seeds released when turbulence is intense are more likely to undergo long distance dispersal [22, 32, 33]. More rarely considered is the lifespan of a fungal spore during transport in the open atmosphere. But in fact spores in flight are exposed to e.g. UV light damage, and may survive for a time that ranges from less than an hour [26] to several weeks [34], and possibly even longer [35]. Spore lifetime directly affects fitness: a spore that dies in the atmosphere will have zero fitness, even if it ultimately settles back to the ground.

The duration of a spore's journey in the atmosphere dictates its chances of survival: spores survive in the atmosphere if they return to the ground during their lifetime. But the duration of the journey for individual spores is inherently unpredictable due to turbulence: two identical spores released from a single sporocarp may take radically different paths [27]. However, the average flight time for a group of spores released simultaneously from the same location may follow a specific pattern, which is often studied in the context of aerosol science (and named residence time or flight time, see e.g. [28]). The flight time of large aerosols (diameter 5 – 20 μm , similar to a typical fungal spore) results from the balance between two opposite forces: gravity causes particles to sediment downward, and turbulence keeps them aloft [28]. Hence for exam-

Reserved for Publication Footnotes

ple residence time for larger particles is shorter [28, 29, 30]. To make the above argument quantitative, aerosol science often assumes that the dynamics has reached an equilibrium because e.g. particles take off from a large area that does not vary in time. But this is not the case for fungi, which are discrete entities, distributed in irregular patches and may produce and release spores at one point in time only. A recent model [31] considers particles released at one time in the idealized case of a vertically infinite neutral atmosphere, i.e. where the intensity of turbulence increases linearly with altitude, and does not change in time. A main conclusion of their idealized model is that the flight time becomes infinitely long when turbulence is stronger than sedimentation. More realistic analyses of spore flight time considering variations with season, geography, and state of the atmosphere, require massive numerical simulations using meteorological data.

By combining state-of-the-art numerical simulations of atmospheric particle transport with simplified models of atmospheric turbulence, and by explicitly considering spore lifespan, we discover the timing of spore liberation dramatically influences the effective reach of viable spores. Manipulating the timing of spore liberation will dramatically influence fitness. We find (i) the average duration of a spore's flight depends on when it is released; by explicitly defining fitness as the fraction of spores that sediment during their lifetime we discover patterns in flight time cause specular patterns in fitness. (ii) Turbulence dominates vertical transport and thus dictates flight time in realistic conditions, reminiscent of previous results limited to idealized transport models. (iii) The cyclical nature of turbulence drives observed patterns in fitness: typically, turbulence is stronger during the day versus at night. The strength and reliability of this diurnal cycle of turbulence varies with geography and season. (iv) When and where the cyclical pattern of turbulence is unreliable, a direct measure of the local intensity of turbulence will be a better guide than time of day to maximise fitness. Results provide a set of testable hypotheses to understand observed patterns of spore release: (1) Releasing spores at specific times of the day is beneficial for species living in regions where the atmosphere cycles regularly. (2) For these species, short-lived spores should be released at night, while long lived spores can be released during the day. (3) Intermittent patterns of spore release may emerge as an adaptation to an environment where the diurnal cycle of turbulence is disrupted.

While atmospheric transport is assumed to be unpredictable, and fungi are assumed to have little control over it, spore discharge itself appears finely tuned to maximize individual fitness [36, 37, 38, 39, 40, 41]. Our results demonstrate that fungi may still maximize one aspect of fitness by strategizing timing of spore release.

Results

The duration of a spore's flight in the atmosphere can be controlled by the timing of spore release. To determine the statistics of spore flight time, we follow the trajectories of many spores released instantaneously from single sites. We model an array of 10 locations in North America (see Supplementary Figure 1 and Supplementary table), releasing groups of 100,000 spores from the first layer of the atmosphere closest to the soil every 3 hours over the course of four different months (January, April, July and October 2014), resulting in a total of 9600 numerical simulations. Our simulations track the Lagrangian trajectories of spores in the atmosphere using meteorological data publicly available from NOAA and

the software HYSPLIT [42, 43, 44, 45, 46], see Materials and Methods and Supplementary information. Particles are modeled as tracers carried across the atmosphere both vertically and horizontally, with a specific gravitational settling velocity. Spores are carried by the large scale wind field, coming from meteorological models, and are additionally kicked and buffeted by turbulent fluctuations. Turbulence is modeled as a correlated stochastic process akin to a simple diffusion, with an effective diffusivity (*eddy diffusivity*) that depends on height. To mimic deposition, spores remaining or returning to the first layer closest to the soil are randomly removed from the simulation and returned to the ground with a constant rate proportional to the deposition velocity. Our simulations focus on the large scales representing the journey of spores that travel in the open air, and do not resolve the details of release and deposition within the canopy. We record the duration of each particle's trajectory in the open air from take off to landing and analyze the statistics of each group of 100,000 spores. We consider deposition velocity equal to sedimentation velocity, as suitable for large particles [28] and we set it to 6 mm/s (corresponding to an equivalent sphere of radius $6\mu\text{m}$ and density equal to the density of water). We follow each group of spores for 6 weeks; by then, most spores have sedimented to the ground; a small fraction of spores (on average about 16%) escapes into the stratosphere and is rapidly carried outside of the computational domain by strong geostrophic winds, see supplementary Figure 2.

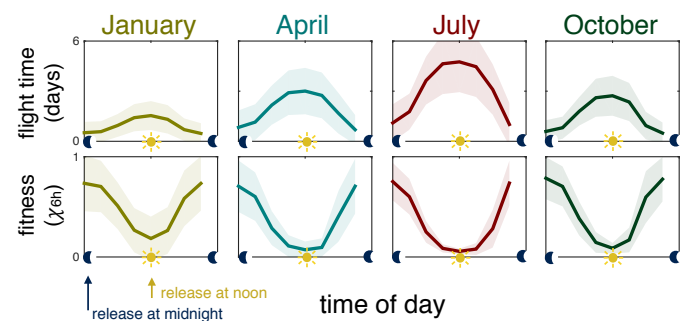


Fig. 1. Spore survival depends on time of liberation. Top row: Average flight time from liberation to deposition as a function of the time of day. Eight take-offs were simulated each day at ten locations for the entire months of January, April, July and October 2014. Bottom row: Fitness χ_{6h} , defined as the fraction of spores deposited within their lifetime τ : $\chi = \int_0^\tau p(t)dt$ with $\tau = 6$ hours.

We find that spore release at different times of the same day results in dramatic oscillations in flight time ranging from less than an hour to several days (Figure 1, top row), consistent with previous results in the context of aerosol science [28]. Longer flight times are observed in the summer (Figure 1, top row), confirming a previously observed seasonal pattern in residence time of abiotic particles [47]. We define one aspect of *fitness* [48] as the fraction of particles deposited within their lifetime τ and indicate it with the symbol χ_τ (w is commonly used for fitness in evolutionary biology but here we reserve the symbol w for velocity, as is standard in the physics literature). Similar to the results for flight time, fitness also undergoes oscillations (Figure 1, bottom row for $\tau = 6$ hours). Note that peaks in flight time correspond to minima in fitness. Indeed, maximum flight times are on the order of several days and in these conditions most of the spores die in flight, since their lifetime is 6 hours. Conversely at night flight times are min-

ima and spore survival is maximum. Hence short-lived spores should be released at night in order to maximize fitness. Similar relationships hold for different choices of lifetime τ , but fitness tends to flatten out for longer lived spores, which can survive even very long flights (see Supplementary Figure 3 for results with $\tau = 2$ days and $\tau = 2$ weeks). Hence timing of spore release only weakly affects survival of long lived spores, which may be released at any time of the day: other aspects of fitness will shape their liberation patterns, for example the need to maximize dispersal range. Demographic variables, and specifically the temporal viability of spores, emerge as critical controls on successful dispersal.

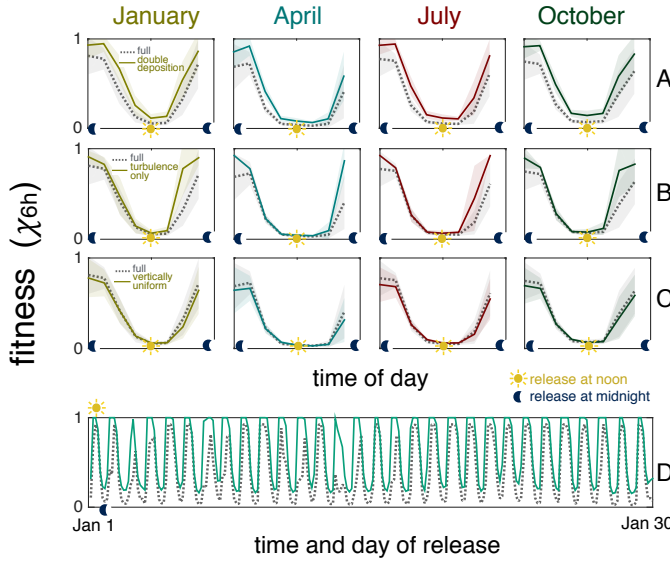


Fig. 2. Turbulence dictates fitness: wind, the details used to model turbulence, and deposition efficiency only slightly affect results. In all panels, grey dotted lines represent fitness averaged across all simulations performed in the same month, as a function of the timing of spore release with $\tau = 6$ hours, computed from the full HYSPLIT simulations described in the text. Gray shading represents the standard deviation of fitness over all simulations. Solid lines represent fitness calculated from: (A) HYSPLIT simulations where the efficiency of deposition is doubled; (B) simplified HYSPLIT simulations without large scale meteorological winds; (C) HYSPLIT simulations with an eddy diffusivity that varies in time but not in z for the entire troposphere; (D) one dimensional finite difference simulations implementing the eddy diffusivity model only (no gravitational settling, no large scale meteorological winds, no horizontal displacement). Note how the model that implements only turbulence reproduces nearly exactly the full model. All simulations start from the same location (10) in Mexico (see Supplementary Table 1).

Oscillations of flight time and fitness are qualitatively robust to small variations of sedimentation and gravitational settling and they will vary quantitatively. Doubling deposition or sedimentation results in shorter flight times and therefore increase in fitness (see Figure 2A and supplementary Figure 4). This result has been previously recognized in the literature for fungal spores (e.g. [29]) and is well known in the context of aerosol science (e.g. [28]). A substantial difference occurs for much larger sedimentation of 6 cm/s (corresponding to a sphere with diameter $40 \mu\text{m}$), where sedimentation dominates the dynamics, as well known for seeds [21] (supplementary Figure 4). In the following we will not further discuss this regime, and focus on the more typical case with spores smaller than $\sim 20 \mu\text{m}$ in diameter. Next, we use our simulations to trace these fitness oscillations back to turbulence.

Flight times and fitness depend mainly on turbulence. Figure 2B shows that fitness is only weakly sensitive to the wind that spores experience along their trajectory because typically, turbulence dominates over vertical wind. Horizontal winds do not affect the vertical dynamics either, because meteorological parameters vary slowly in space. To test the robustness of our turbulence model, we implemented two closures for subgrid fluctuations (see Materials and Methods). Both closures result in the same qualitative results (supplementary Figure 5). We next tested whether the exact profile of these phenomenological expressions is relevant for understanding the mechanism. To this end, we further simplified the HYSPLIT simulation by using a vertically uniform eddy diffusivity resulting from the average over the entire column; the results accord well with the full numerical simulation (Figure 2C). These results suggest that the intensity of turbulence dictates fitness almost entirely. To test this idea, we temporarily left the HYSPLIT framework, and modeled the rate of change of spore concentration over the vertical direction, using solely the turbulent model extracted from HYSPLIT (Eulerian eddy diffusivity model, see Materials and Methods). Fitness is well approximated by this bare bones model, confirming that the intensity of turbulence is the single major parameter dictating fitness.

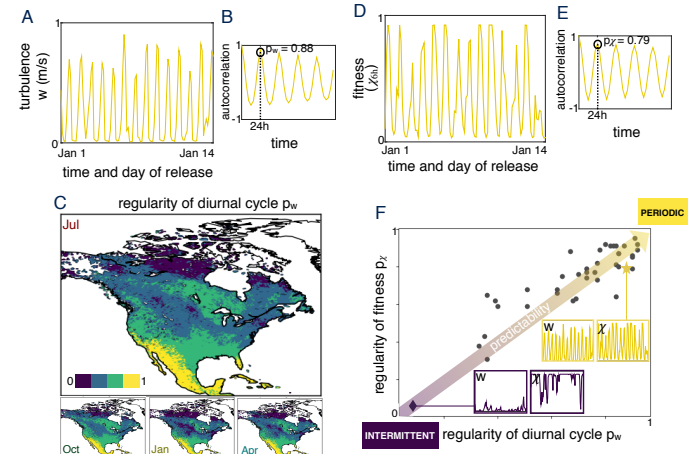


Fig. 3. Atmospheric turbulence undergoes a diurnal cycle that varies according to geography and season. (A) Magnitude of vertical turbulent velocity (w) during two weeks in January in Mexico (in 2014 at location #10 in Mexico, Supplementary Table 1). (B) The corresponding autocorrelation function $\langle (w(t) - \bar{w})(w(t+t') - \bar{w}) / \sigma_w^2 \rangle$, where $\langle \cdot \rangle$ denotes average over 10 days. We define an index p_w (for periodicity) measuring the autocorrelation at 24h, a measure of the reliability of the diurnal cycle. For a perfectly periodic signal $p_w = 1$, whereas for an intermittent signal $p_w = 0$. (C) Map of p_w computed from meteorological datasets, color coded from yellow (regular) to purple (intermittent), for the entire North American continent and different seasons. (D) Regular oscillations of fitness χ_{6h} and (E) its autocorrelation $\langle (\chi_{6h}(t) - \bar{\chi}_{6h})(\chi_{6h}(t+t') - \bar{\chi}_{6h}) / \sigma_{\chi}^2 \rangle$ calculated for the same simulations and as described for turbulence in panel (B). The autocorrelation of χ_{6h} at 24h defines the index p_{χ} for fitness, similar to the index p_w for velocity. (F) Index p_{χ} for fitness at 6 hours is positively correlated to index p_w for turbulence. The lower left corner corresponds to highly intermittent cases (purple diamond is location #1 in Canada in January), while the top right corresponds to extremely regular conditions (yellow star is location #10 in Mexico, shown in panels A,D).

Oscillations in fitness are caused by alternations between strong turbulence during the day and weak turbulence during the night. During the day the sun warms up the atmosphere and soil, the soil warming up faster than the air. The soil in turn warms the lowest layers of the atmosphere and be-

cause warm air tends to rise, it powers thermal convection and intense turbulence. Releasing spores in these conditions will cause them to be carried in the upper layers of the atmosphere, resulting in long flights during the day. Conversely, during the night, the lack of sun causes fast cooling of the soil and hence of the lowest layers of air, often causing stable stratification and weak turbulence. Spores released in these stable conditions never reach large altitudes and return to the ground faster. To understand where this diurnal cycle may be strongest, we extracted from the full meteorological dataset the intensity of turbulent fluctuations: we indicate with w the standard deviation of fluctuations in vertical air speed, mediated in height and computed within HYSPLIT. Larger values of w correspond to greater intensities of turbulent fluctuations. In Figure 3A we show w measured from location #10 in Mexico during the first 2 weeks of January. Turbulence displays regular diurnal oscillations over the entire period. To quantify the consistency of this diurnal cycle, we define an index p_w as the autocorrelation of turbulence w at 24 h (Figure 3B). This index ranges from 1 for a perfectly periodic signal to 0 for an irregular or *intermittent* signal. We next compute p_w for the entire North American continent for the months of January, April, July and October. We approximate w as the standard deviation of the convective velocity, a parameter that is available from the meteorological dataset, and does not require HYSPLIT. Although the diurnal cycle is widespread, its consistency or reliability varies with geography and season (Figure 3C). To verify whether the diurnal cycle of turbulence affects fitness, we compute a second index p_χ analogous to p_w and measuring periodicity of fitness for each of the 10 starting locations and 4 different months we simulated previously. Figure 3D-E shows one example of fitness χ and its autocorrelation defining p_χ , for the same location/weeks illustrated in Figure 3A-B. Next we correlate p_w with p_χ and we find that periodicity of turbulence correlates well with periodicity of fitness (Figure 3F). This correlation is extremely useful, as the index p_w can be computed from meteorological data, and this index can be used to estimate p_χ with no need of simulating spore trajectories. This analysis suggests that when and where turbulence is periodic $p_w \sim 1$, fitness is also periodic $p_\chi \sim 1$ and in these regions marked in yellow/green in Figure 3C, releasing spores at specific times of the day may be a strategy used by fungi to maximize fitness.

However, releasing spores at the same time every day may not always be a good strategy; if turbulence is difficult to predict, rhythmic patterns of spore release may not maximize fitness. In our pool of simulations, the weakest diurnal cycle is found in location #1 in Canada during the month of January (Figure 4A-D). Although January is not the typical season for sporulation, we use this simulation as an extreme example to illustrate maximum intermittency of turbulence. In this simulation, both turbulence and fitness vary irregularly from day to day and the indices p_w and p_χ are close to zero (purple diamond in Figure 3D; Figure 4B,D). Every day is different. Even in environments where there is no periodicity, intense turbulence at liberation causes spores to be lifted up in altitude and fitness to plummet. This is exemplified in our most intermittent simulation, where negative fluctuations in fitness (troughs in Figure 4C) often occur when turbulence is intense (peaks in Figure 4A). To maximize fitness in intermittent environments, species may still evolve to liberate spores when turbulence is weak, but by evolving to measure turbulence directly.

To test this idea we compare two alternative models. In the first model, we consider fitness as a function of time of day (Figure 1 bottom row). In the second model, we con-

sider fitness as a function of turbulence intensity (Figure 4E). In both cases, we perform non-linear regressions to obtain a function f that predicts fitness $\chi = f(t)$ as a function of time of the day, and a second function g that predicts fitness $\chi = g(w)$ as a function of turbulence (see Materials and Methods). We then compute the mean square error for the prediction in the two cases and for each of the 40 simulated locations and months, $\text{error}(t) = \sqrt{\langle [f(t) - \chi]^2 \rangle}$ and $\text{error}(w) = \sqrt{\langle [g(w) - \chi]^2 \rangle}$. We find that turbulence intensity predicts fitness more accurately than time of the day when the cycle is disrupted (purple region Figure 4F); time of the day and turbulence are nearly equally accurate in predicting fitness when the cycle is regular ($p_w \gtrsim 0.8$, yellow region Figure 4F). In intermittent conditions, spores should be liberated whenever turbulence intensity is low regardless of whether it is day or night. This is especially true for our most intermittent simulation, which is an outlier (purple diamond in Figure 4F), but is also relevant to several other simulations where releasing spores according to turbulence may increase fitness by about 0.17 for example April in Colorado and July in Wisconsin.

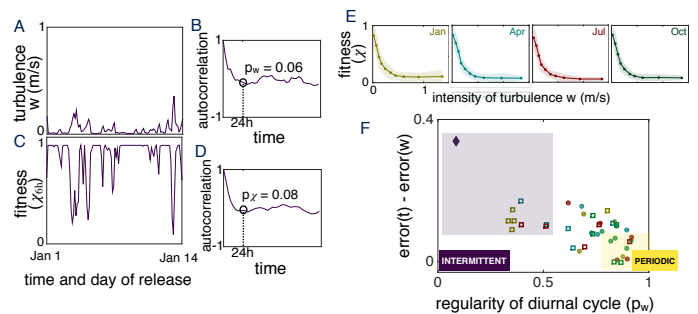


Fig. 4. Releasing spores at the same time every day is not efficient when intensity of turbulence is intermittent. (A) Magnitude of vertical turbulent velocity w , (B) its autocorrelation function; (C) Fitness χ_{6h} and (D) its autocorrelation. Panels A-D are the same as Figure 3 A-B-D-E, for the same two weeks but a different location (#1 in Canada, see Supplementary Table 1). (E) Fitness as a function of turbulence intensity, all simulations are pooled together by month. (F) Difference between error when predicting fitness according to turbulence *vs* time of the day for each of the 40 simulated months. Squares correspond to the Northern locations (#2 #4 #6 #7 #10) and dots the Southern Locations; months are color coded as in (E). The error is defined as $\sqrt{\langle [f(t) - \chi]^2 \rangle}$ for time of the day and $\sqrt{\langle [g(w) - \chi]^2 \rangle}$ for turbulence. Note how turbulence intensity is a better predictor of fitness than time of the day for small values of p_w corresponding to intermittent conditions (purple shaded area). Whereas time of the day and turbulence are nearly equally accurate in predicting fitness when the atmosphere cycles regularly between weak and intense turbulence (yellow shaded region).

Discussion

Our results demonstrate that time of the day when spores are released dramatically affects their fitness. Spores released during the day tend to be transported higher up in the atmosphere, and return to the ground after several days. But many spores can only survive few hours in the open atmosphere, and would die before returning to the ground. Hence, we predict that to maximize survival short-lived spores should be typically launched at night. *Mycosphaerella fijiensis* [2, 3], and *Giberella zeae* [6, 7] release spores preferentially at night, and measures of their survival to UV light damage suggest that their lifetime in the open atmosphere is indeed extremely short, consistent with our prediction [49, 50, 51, 52]. But why are some species releasing spores during the day? Our results show that fitness peaks at night for short-lived

spores; however, fitness flattens out as spores are more long lived (see Supplementary Figure 3 for results with $\tau = 2$ weeks and $\tau = 2$ days). In other words, spores that are adapted to survive in the atmosphere for weeks can be released at any time of the day including when turbulence is maximum during the day. Because survival in the air is not limiting, long lived spores may be released in conditions that maximize a different aspect of fitness, for example, distance travelled. In order to maximize distance travelled, these spores should be released in strong turbulent conditions, typically found during the day. Consistent with this hypothesis, asexual spores of *Botrytis cinerea* [53, 54], *Alternaria spp.* [55], *Cladosporium spp.* [55, 56] preferentially release spores during daytime hours.

Releasing spores at specific time of the day modulates the expected fraction of spores surviving the journey, suggesting that fungi may tie spore liberation to an internal clock. Interestingly, it is known that spore production in *Neurospora crassa* is indeed regulated by the circadian clock [57, 58], but whether this may provide any selective advantage has been hitherto unclear. Our results suggest that producing spores at certain times of the day may be instrumental to release them at times that maximize chances of survival.

A clock is not always a useful predictor of fitness: in cases where the atmospheric cycle is disrupted, turbulence varies irregularly, and releasing spores at the same time every day can lead to massive losses. In regions where the cycle is disrupted, short lived spores should be released intermittently, whenever turbulence is weak, whereas long lived spores can be released in conditions of intense turbulence. Intermittent patterns of spore liberation do occur [18], however what features of the environment dictate spore release is still poorly understood [17]. The abscission of asexual spores of, e.g., *Cochliobolus heterostrophus* (syn. = *Helminthosporium maydis*), whose spores are among those considered to be capable of withstanding atmospheric conditions experienced during continental-scale dispersal [34], occurs only when wind velocity exceeds 10 m/s [59]. This is consistent with our hypothesis, because large air speed close to a substrate is usually associated to intense turbulent wind gusts.

Whether a clock-based or a sensation-based strategy is more effective, depends on the environment that a species is adapted to. To compare these two alternative strategies, we introduced the parameter p_w which distinguishes between regions with regular *vs* intermittent atmospheric conditions. This analysis provides a testable hypothesis for the emergence of intermittent *vs* regular spore release. If patterns of spore liberation are shaped by the need to maximize spore survival in the atmosphere, species adapted to regions where the diurnal cycle is strong ($p_w > 0.8$ in our test case) will release spores according to their internal clock. Whereas species adapted to an environment with a weak diurnal cycle ($p_w < 0.8$ in our test case) are more likely to liberate spores intermittently in response to environmental conditions that measure turbulence intensity. The value of p_w that marks this transition will vary from species to species, according to spore morphology and longevity, but the qualitative pattern is robust. To test this hypothesis, the patterns of spore liberation must be monitored in the field, along with the genetic structure of the population and spore morphology and longevity in the atmosphere. What species favors one strategy over the other will determine how spore liberation will shift

in response to environmental changes including global change.

Spore dispersal is generally regarded as dangerous and fundamentally wasteful. Our results demonstrate that although fungi do lose control over individual spores, they can still maximize fitness in the atmosphere by manipulating the timing for spore release. Indeed, the timing for spore liberation dictates the fraction of spores that survive their journey in the open atmosphere. In other words, the ensemble statistics of spore flight time keeps memory of the initial conditions that spores meet when they first reach the open air. These results partially reconcile two contrasting aspects of fungal spore dispersal: microscopic optimization *vs* large scale uncertainty. On the one hand, at micron to cm scales, fungi evolved fascinating adaptations to maximize efficiency of the microscopic mechanism of discharge (reviewed in [41]). The ascomycetes, the most numerous phylum in the higher fungi, fire sexual spores from a pressurized cell which is finely regulated to minimize dissipation [36, 37, 38, 39, 40]. The basidiomycetes, including ~ 40000 mushroom-forming species, eject spores through a surface tension catapult that achieves precise control of spore range right after discharge [60, 61, 62, 63, 64, 65, 66]. These adaptations indicate that spore dispersal is under considerable selective pressure. But this idea is at odds with the fact that, once spores reach dispersive airflows, their fate is dictated by a series of stochastic events and appears entirely out of control. Fungi acknowledge uncertainty by producing a large number of propagules, making fungal migration extremely different from the ordered migration of mammals and fundamentally wasteful [67]. Here we show that, in addition, fungi may use their exquisite microscopic control to release spores when their chances of survival in the atmosphere are highest.

Lagrangian simulations with meteorological data using HYSPLIT

To compute the statistics of flight times, we follow many particles released from a given location at different times using the Hybrid Single Particle Lagrangian Integrated Trajectory (HySPLIT) model [68] an open source code developed at the Air Resource Laboratory of the National Ocean and Atmospheric Administration (ARL-NOAA) in the US. We modeled spores as passive tracers with an additional gravitational settling velocity. Spores are transported by the wind, whose velocity is obtained from meteorological datasets on a large scale grid with resolution 32 km, turbulence on smaller scales is modeled as a correlated stochastic process, so spore trajectories can be computed through a Langevin equation:

$$\frac{d\mathbf{P}(t)}{dt} = \mathbf{V}_{\text{meteo}}[\mathbf{P}(t), t] + \mathbf{V}'[\mathbf{P}(t), t] + \mathbf{V}_G. \quad [1]$$

where \mathbf{P} is the three dimensional instantaneous location of a spore, $\mathbf{V}_{\text{meteo}}$ is the large-scale wind velocity from the North American Regional Reanalyses (NARR) [69]; \mathbf{V}' is a realization of the stochastic turbulent fluctuation [70] and \mathbf{V}_G the gravitational settling velocity. NARR is an extended dataset of meteorological variables on a regular grid covering the whole North American continent resulting from a matching procedure between outputs of numerical models and sparse observations of many atmospheric variables. NARR data are given on a Lambert conformal grid with 309 x 237 horizontal points and 24 levels on a vertical pressure-sigma coordinates system. The nominal horizontal resolution is 32 km. Starting from 1979 to today the state of the atmosphere is available

at a time resolution of 3 hours. The variance of turbulent fluctuations in the vertical direction depend on height and is modeled with semi-empirical expressions that vary with the state of the atmosphere, i.e. stable *vs* unstable (see Supplementary Information for details, [71, 72]). The specific choice for the closure as well as their dependence on altitude only weakly affect fitness (see Supplementary information). Spores sediment with a constant downward velocity. Qualitative results are robust for sedimentation velocities of the order of 1 cm/s. As a reference, this value of sedimentation velocity corresponds to a sphere with the density of water and diameter 18 μm . Results vary considerably for spores sedimenting 10 times faster (see Supplementary Information). Finally, dry deposition to the ground is computed assuming that the flux of spores $j(\mathbf{x}, t)$ to the ground is proportional to concentration of spores close to the soil $\theta(\mathbf{x}, t)$: $j(\mathbf{x}, t) = V_d \theta(\mathbf{x}, t)|_{z=0}$, where V_d was taken equal to the gravitational settling, as appropriate for spherical particles larger than about 1 μm [28]. A more detailed modeling of deposition on the canopy including dependence on spore shape is left for future studies. Figure 2 shows that deposition velocities affect fitness quantitatively, but do not affect the qualitative patterns. In our model, the gravitational/deposition velocity is the only parameter of the dynamics that depends on the fungal species. Wet deposition may decrease the flight time in daytime releases, but does not change the general conclusions unless fungi are able to release spores right before rain. There is some evidence that this may be true for some species, and we will treat this fascinating possibility elsewhere.

One dimensional model of spore transport

In the Eulerian framework, the concentration of passive tracers advected by a short-correlated velocity field in one dimension follows the well-known Fokker–Plank equation $\partial_t \theta(z, t) = \partial_z [D(z) \partial_z \theta] + v_D \partial_z \theta$, see e.g. [73, 27], where $\theta(z, t)$ is the average concentration of spores at altitude z and time t ; $D(z)$ is the vertical eddy diffusivity, for which we use the closures implemented in the HYSPLIT simulations (see Supplementary information), and v_D is the sedimentation velocity. We compared fitness obtained through this simplified one-dimensional model that neglects the horizontal dynamics entirely to the results of the full HYSPLIT model. The one dimensional model captures well the importance of stability in determining fitness, and reproduces the oscillations observed in the full simulations. We impose reflecting boundary conditions at the top of the domain (25 km), and we remove a fraction of spores localized at $z < 50$ m according with the deposition velocity, as done by the HYSPLIT model. We adopt a finite volume scheme with regular cells of $\Delta z = 5$ m and a Runge-Kutta algorithm of fourth order for time marching, with time step Δt chosen according to the Courant criterion: $\Delta t = \min_{D_i} \frac{\Delta z^2}{8 D_i}$ where

$D_i = D(z_i)$ is the eddy diffusivity evaluated at the center of the i -th vertical cell.

Regression

To determine whether time of the day or vertical turbulence hold the most reliable information about fitness, we perform non linear regression using Gaussian processes [74, 75, 76]. This is a non-parametric method for regression, with the advantage that the fitting function can be represented as an infinite sum of basic functions hence making the procedure extremely flexible. We target a function that predicts fitness χ from input data x , where x represents either time of day or turbulent intensity at spore release. χ is assumed to be a Gaussian random variable, with mean $\bar{\chi} = f(x)$ and variance β^{-1} . A kernel function is defined to quantify distances between different input points, here we use a Gaussian kernel $k(x_i, x_j) = e^{-||x_i - x_j||^2 / (2\pi\lambda^2)}$. Given a training set $(\mathbf{x}, \chi) = (x_1, \dots, x_N, \chi_1, \dots, \chi_N)$, the probability distribution $p(\chi_{N+1} | \chi)$ for the value of χ associated to a test data x_{N+1} , conditioned to the previous observations, is a gaussian with mean

$$f(x_{N+1}) = \mathbf{k}^T \underline{\underline{C}}^{-1} \chi$$

and variance

$$\sigma^2(x_{N+1}) = c - \mathbf{k}^T \underline{\underline{C}}^{-1} \mathbf{k}$$

where $C(x_n, x_m) = k(x_n, x_m) + \beta^{-1} \delta_{nm}$; $c = k(x_{N+1}, x_{N+1}) + \beta^{-1}$ and $\mathbf{k} = k(x_{N+1}, x_n)$ and $n, m \in (1, N)$. We choose the parameters of the model, λ and β , so as to minimize the generalization error using cross validation. We split our 9600 simulations (10 locations \times 4 months \times 30 days \times 8 releases per day) in 240 test points (1 location \times 1 month \times 30 days \times 8 releases per day) and 9630 training points (the rest). We use a random subsample of 1000 (for t) and 1500 (for w) simulations from the training set to train the algorithm and use it to predict the test set. We compute the generalization error on the test data and we repeat the procedure over the 40 different ways to split the dataset in test and training, and average to obtain the test error. We repeat the procedure varying systematically the parameters and identify the region in the parameter space that provide minimum test error. The difference in the generalization error, defined as $(\chi - f(x))^2$, for x = time of day and x = turbulence intensity, with the parameters selected as above, is plotted in Figure 4F.

ACKNOWLEDGMENTS. This work was supported by the Agence Nationale de la Recherche Investissements d’Avenir UCA^{JEDI} #ANR-15-IDEX-01 and CNRS PICS “2FORECAST”, by the Thomas Jefferson Fund, a program of FACE. We acknowledge support for computational resources from INFN and CINECA. The authors gratefully acknowledge the NOAA Air Resources Laboratory (ARL) for the provision of the HYSPLIT transport and dispersion model. NCEP Reanalysis data were provided by the NOAA/OAR/ESRL PSD, Boulder, Colorado, USA, from their Web site at <https://www.esrl.noaa.gov/psd/>

1. DA Glawe. “The powdery mildews: a review of the world’s most familiar (yet poorly known) plant pathogen”. *Annu. Rev. Phytopathol.* 46:27–51 (2008)
2. DS Meredith, JS Lawrence, ID Firman. “Ascospore release and dispersal in black leaf streak disease of bananas” *Trans Br Mycol Soc.* 60:547–554 (1973)
3. L Jacome, P Lepoivre, D Marin, R Ortiz, R Romero, VJ Escalant. “Mycosphaerella Leaf Spot Diseases of Bananas: Present Status and Outlook”. *Proceedings 2nd International workshop on Mycosphaerella leaf spot diseases* (2002)
4. JX Zhang, WGD Fernando, AG Xue. “Daily and seasonal spore dispersal by *Mycosphaerella pinodes* and development of *Mycosphaerella blight* of field pea”. *Can J Bot* 83:302–310 (2005)
5. D Meredith, J Lawrence, I Firman. “Ascospore release and dispersal in black leaf streak disease of bananas (*Mycosphaerella fijiensis*)”. *T Brit Mycol Soc* 60:547–554 (2009)
6. TC Paulitz. “Diurnal release of *Ascospores* by *Gibberella zeae* in Inoculated Wheat Plots”. *Plant Disease* 80:674–678 (1996)
7. J Gilbert, SM Woods and U Kromer. “Germination of *Ascospores* of *Gibberella zeae* After Exposure to Various Levels of Relative Humidity and Temperature” *Phytopathol* 98:504–508 (2008)
8. V Rossi, I Ponti, M Marinelli, S Giosué, R Bugiani. “Environmental factors influencing the dispersal of *Venturia inaequalis* ascospores in the orchard air”. *J Phytopathol* 149:11–19 (2001)
9. JM Hirst, OJ Stedman. “The epidemiology of apple scab (*Venturia inaequalis*) (cke.) Wint.) III. The supply of ascospores.” *Ann Appl Biol* 50:551–567 (1962)
10. GS Gilbert, DR Reynolds. “Nocturnal Fungi: Airborne Spores in the Canopy and Understory of a Tropical Rain Forest” *Biotropica*, 37:462–464 (2005)
11. JA Huffman, B Sinha, RM Garland, A Snee-Pollmann, SS Gunthe, P Artaxo, ST Martin, MO Andreae, U Poschl. “Size distributions and temporal variations of bi-

- ological aerosol particles in the Amazon rainforest characterized by microscopy and real-time UV-APS fluorescence techniques during AMAZE-08" *Atmos. Chem. Phys.* 12:11997–12019 (2012)
12. YJ Huang, BDL Fitt, M Jedryczka, S Dakowska. "Patterns of ascospore release in relation to phoma stem canker epidemiology in England (*Leptosphaeria maculans*) and Poland (*Leptosphaeria biglobosa*)". *Eur J Plant Pathol* 111:263 – 277 (2005)
 13. XW Guo, W Fernando. "Seasonal and diurnal patterns of spore dispersal by *Leptosphaeria maculans* from canola stubble in relation to environmental conditions". *Plant Dis* 89:97–104 (2005)
 14. D Savage, MJ Barbetti, WJ MacLeod, MU Salam, M Renton. "Temporal Patterns of Ascospore Release in *Leptosphaeria maculans* Vary Depending on Geographic Region and Time of Observation" *Microb Ecol* 65: 584–592 (2013)
 15. R Khangura, J Speijers, MJ Barbetti, MU Salam, AJ Diggle. "Epidemiology of Black-leg (*Leptosphaeria maculans*) of Canola (*Brassica napus*) in Relation to Maturation of Pseudothecia and Discharge of Ascospores in Western Australia". *Phytopathology* 97:1011–1021 (2007)
 16. DC McGee, RW Emmet. "Black leg (*Leptosphaeria maculans* (desm.) Ces. Et de not.) of rapeseed in Victoria: crop losses and factors which affect disease severity". *Aust J Agric Res* 28:47–51 (1977)
 17. AM Jones, RM Harrison. "The effects of meteorological factors on atmospheric bioaerosol concentrations – a review" *Science Tot. Environ.* 326:151–181 (2004)
 18. DE Aylor. "The role of intermittent wind in dispersal of fungal pathogens" *Annu Rev Phytopathol* 28:73–92 (1990)
 19. DE Aylor, RG Lukens. "Liberation of *Helminthosporium maydis* spores by wind in the field". *Phytopathology* 64: 1136–1138 (1974)
 20. J Rotem. "The Genus *Alternaria*: Biology, Epidemiology, and Pathogenicity". American Phytopathological Society, St Paul, USA (1994)
 21. R Nathan, GG Katul, G Bohrer, A Kuparinen, MB Soons, SE Thomson, A Trakhtenbrot, HS Horn. "Mechanistic models of seed dispersal by wind". *Theor Ecol* 4:113 (2011)
 22. D Savage, MJ Barbetti, MJ MacLeod, MU Salam, M Renton. "Seasonal and Diurnal Patterns of Spore Release Can Significantly Affect the Proportion of Spores Expected to Undergo Long-Distance Dispersal". *Fungal Microb* 63:578 (2012)
 23. D Savage, MJ Barbetti, MJ MacLeod, MU Salam, M Renton. "Timing of propagule release significantly alters the deposition area of resulting aerial dispersal." *Divers Distrib* 16:288–299 (2010)
 24. J Boreson, AM Dillner, J Peccia. "Correlating bioaerosol load with PM2.5 and PM10cf concentrations: a comparison between natural desert and urban-fringe aerosols". *Atmospheric Environment* 38:6029–6041 (2004)
 25. R Jaenicke. "Abundance of Cellular Material and Proteins in the Atmosphere" *Science* 308:73 (2005)
 26. V Norros, E Karhu, J Nórdén, AV Vahatalo, O Ovaskainen. "Spore sensitivity to sunlight and freezing can restrict dispersal in wood decay fungi" *Ecol and Evol.* 5:3312–3326 (2015)
 27. G Falkovich, C Gawedzki, M Vergassola. "Particles and fields in fluid turbulence". *Rev Mod Phys* 73:913–975 (2001)
 28. SH Friedlander. *Smoke, dust and haze. Fundamentals of aerosol dynamics.* Oxford University Press, Oxford, Second Edition (2000)
 29. B Bolin, G Aspling and C Persson. "Residence time of atmospheric pollutants as dependent on source characteristics, atmospheric diffusion processes and sink mechanisms" *Tellus* 26:185–195 (1974)
 30. C Denjean, F Cassola, A Mazzino, S Triquet, S Chevaillier, N Grand, T Bourrianne, G Monboisse, K Sellegrì, A Schwarzenböck, E Freney, M Mallet and P Formenti. "Size distribution and optical properties of mineral dust aerosols transported in the western Mediterranean". *Atmos Chem Phys* 16:1081–1104 (2016)
 31. S Belan, V Lebedev, G Falkovich. "Particle Dispersion in the Neutral Atmospheric Surface Layer" *Boundary Lay. Meteor.* 159:23–40 (2016)
 32. DE Aylor. "Biophysical scaling and the passive dispersal of fungus spores: relationship to integrated pest management strategies" *Agric. Forest Meteorol.* 97:275–292 (1999)
 33. O Tackenberg, P Poschlod, S Kahmen. "Dandelion Seed Dispersal: The Horizontal Wind Speed Does Not Matter for Long Distance Dispersal - it is Updraft!" *Plant Biol* 5:451–454 (2003)
 34. CC Mundt, KE Sackett, LD Wallace, C Cowger and JP Dudley. "Long-Distance Dispersal and Accelerating Waves of Disease: Empirical Relationships" *Amer nat* 173:456–466 (2009)
 35. P DasSarma and S DasSarma. "Survival of microbes in Earth's stratosphere" *Curr. Opin. in Microbiol.* 43:24–30 (2018)
 36. M Roper, R Pepper, MP Brenner, A Pringle. "Explosively launched spores of ascomycete fungi have drag minimizing shapes". *PNAS* 105:20583 (2008)
 37. J Fritz, A Seminara, M Roper, A Pringle, MP Brenner. "A natural O-ring optimizes the dispersal of fungal spores". *J. R. Soc. Interface* 10:20130187 (2013)
 38. M Roper, A Seminara, M Bandi, A Cobb, H Dillard, A Pringle. "Dispersal of fungal spores on a cooperatively generated wind". *PNAS* 107:17474 (2010)
 39. F Trail, A Seminara. "The mechanism of ascus firing: merging biophysical and mycological viewpoints". *Fungal Biol. Rev.* 28:70–76 (2014)
 40. A Pringle, MP Brenner, J Fritz, M Roper, A Seminara. "Reaching the wind: boundary layer escape as a constraint on ascomycete spore dispersal". In *The Fungal Community: Its Organization and Role in the Ecosystem*, ed. J Dighton, JF White, pp. 309–20. Boca Raton, FL: CRC. 4th ed (2017)
 41. M Roper and A Seminara. "Mycofluidics: the fluid dynamics of fungal adaptations" *Annual Rev. Fluid Dyn.* 51:511–538 (2019)
 42. F Mesinger et al "North American Regional Reanalysis" *Bull. Am. Meteorol. Soc* 87:343–360 (2006)
 43. RR Draxler, GD Rolph. "HYSPLIT (HYbrid Single-Particle Lagrangian Integrated Trajectory)" Model access via NOAA ARL READY Website (<http://www.arl.noaa.gov/ready/hysplit4.html>). NOAA Air Resources Laboratory, Silver Spring, MD. (2003)
 44. GD Rolph. "Real-time Environmental Applications and Display sYstem (READY)" Website (<http://www.arl.noaa.gov/ready/hysplit4.html>). NOAA Air Resources Laboratory, Silver Spring, MD (2003)
 45. RR Draxler, GD Hess "An overview of the HYSPLIT₄ modelling system for trajectories, dispersion and deposition". *Aust. Met. Mag.* 47:295–308 (1998)
 46. RR Draxler, GD Hess. "Description of the HYSPLIT₄ modeling system" NOAA Technical Memorandum ERL ARL 224 (1997)
 47. Y Balkanski, DJ Jacob, GM Gardiner, WC Graustein and KK Turekian "Transport and Residence Times of Tropospheric Aerosols Inferred from a Global Three-Dimensional Simulation of ²¹⁰Pb." *Journ. Geophys. Res.* 98,20.573–20.586 (1993)
 48. A Pringle, JW Taylor. "The fitness of filamentous fungi" *TRENDS in Microbiology* 10 (2002)
 49. M Parnell, PJA Burt, K Wilson. "The influence of exposure to ultraviolet radiation in simulated sunlight on ascospores causing Black Sigatoka disease of banana and plantain". *Intern Journ Biometeor* 42: 22–27 (1998)
 50. S Robert, V Ravigné, MF Zapater, C Abadie, J Carlier. "Contrasting introduction scenarios among continents in the worldwide invasion of the banana fungal pathogen *Mycosphaerella fijiensis*" *Mol Ecol* 21:1098–114 (2012)
 51. S Inch, WGD Fernando, J Gilbert "Seasonal and daily variation in the airborne concentration of *Gibberella zeae* (Schw.) Petch spores in Manitoba". *Canad Journ Plant Pathol* 27: 357– 363 (2005)
 52. SL Maldonado-Ramirez, DG Schmale, EJ Shields, GC Bergstrom. "The relative abundance of viable spores of *Gibberella zeae* in the planetary boundary layer suggests the role of long-distance transport in regional epidemics of *Fusarium head blight*". *Agric and For Meteorol* 132: 20–27(2005)
 53. GA Chastagner, JM Ogawa, BT Manji. "Dispersal of conidia of *Botrytis cinerea* in tomato fields". *Phytopathol* 68:1172–1176 (1978)
 54. WFT Hartill. "Aerobiology of *Sclerotinia sclerotiorum* and *Botrytis cinerea* spores in New Zealand tobacco crops". *New Zealand Journal of Agricultural Research* 23:259–262 (1980)
 55. DJ O'Connor, M Sadys, CA Skjoth, DA Healy, R Kennedy, JR Sodeau. "Atmospheric concentrations of *Alternaria*, *Cladosporium*, *Ganoderma* and *Didymella* spores monitored in Cork (Ireland) and Worcester (England) during the summer of 2010". *Aerobiologia* 30:397–411 (2014)
 56. SM Pady, CL Kramer, R Clary. "Periodicity in Spore Release in *Cladosporium*" *Mycologia* 61:87–98 (1969)
 57. C Heintzen, Y Liu. "The *Neurospora crassa* Circadian Clock". *Advances in Genetics* 58:25–66 (2007)
 58. ML Springer. "Genetic control of fungal differentiation: The three sporulation pathways of *Neurospora crassa*" *Bioessays* 15:365–374 (1993)
 59. DE Aylor. "Force Required to Detach Conidia of *Helminthosporium maydis*". *Plant Physiol* 55:99–101 (1975)
 60. AHR Buller. "Researches on Fungi" 1–7. London: Longmans, Green, and Co (1909–1950)
 61. CT Ingold. "Spore Discharge in Land Plants". Oxford: Clarendon (1939)
 62. J Turner, J Webster. "Mass and momentum transfer on the small scale: How do mushrooms shed their spores?". *Chem. Eng. Sci* 46:1145–49 (1991)
 63. A Pringle, S Patek, M Fischer, J Stolze, N Money. "The captured launch of a ballistospore". *Mycologia* 97:866–71 (2005)
 64. X Noblin, S Yang, J Dumais. "Surface tension propulsion of fungal spores". *J. Exp. Biol.* 212:2835–43 (2009)
 65. JL Stolze-Rybczynski, Y Cui, M Henry, H Stevens, D Davis, MWF Fischer, NP Money. "Adaptation of the spore discharge mechanism in the Basidiomycota". *PLOS ONE* 4:e4163 (2009)
 66. F Liu, RL Chavez, SN Patek, A Pringle, JJ Feng, CH Chen. "Asymmetric drop coalescence launches fungal ballistospores with directionality". *J. R. Soc. Interface* 14:20170083 (2017)
 67. S Nagarajan, DV Singh. "Long-distance dispersion of rust pathogens". *Annu. Rev. Phytopathol.* 28:139–53 (1990)
 68. AF Stein, RR Draxler, GD Rolph, BJB Stunder, MD Cohen, F Ngan. "NOAA's HYSPLIT atmospheric transport and dispersion modeling system". *Bull. Amer. Meteor. Soc.* 96: 2059–2077 (2015)
 69. F Mesinger, G DiMego, E Kalnay, K Mitchell, and Coauthors. "North American Regional Reanalysis". *Bull Amer Meteorol Soc* 87: 343–360 (2006)
 70. JD Wilson, BJ Legg, DJ Thomson. "Calculation of particle trajectories in the presence of a gradient in turbulent velocity variance". *B. Layer Meteorol.* 27: 163–169 (1983)
 71. LH Kantha, CA Clayson. "Small Scale Processes in Geophysical Fluid Flows" International Geophysics Series 67, Academic Press, San Diego, CA, 883 pp. (2000)
 72. ACM Beljaar, AAM Holtlag. "Flux parameterizations over land surfaces for atmospheric models". *J. Appl. Meteorol.* 30: 327–341 (1991)
 73. A Okubo, SA Levin. "A theoretical framework for data analysis of wind dispersal of seeds and pollen". *Ecology* 70:329–338 (1989)
 74. DJC MacKay. *Introduction to Gaussian processes.* In C. M. Bishop (Ed.), *Neural Networks and Machine Learning*, pp. 133–166. Springer. (1998)
 75. CM Bishop. "Pattern recognition and machine learning", Springer (2006).
 76. CE Rasmussen and CKI Williams. "Gaussian Processes for Machine Learning", MIT Press (2006)

Supplementary Information for: “Timing of fungal spore release dictates survival to atmospheric transport”

Daniele Lagomarsino Oneto,¹ Jacob Golan,² Anne Pringle,² Andrea Mazzino,³ and Agnese Seminara⁴

¹*Université Côte d’Azur, Institut de Physique de Nice, 06108, Nice France*

²*Departments of Botany and Bacteriology,*

University of Wisconsin-Madison, Madison, WI, USA

³*Department of Civil, Chemical, and Environmental Engineering,*

University of Genova and INFN, via Montallegro 1, 16145 Genova, Italy

⁴*CNRS and Université Côte d’Azur,*

Institut de Physique de Nice, Parc Valrose, 06108, Nice

Abstract

This document includes the following Supplementary Information for the paper: “Timing of fungal spore release dictates survival to atmospheric transport”

I Lagrangian simulations with weather data using HYSPLIT



Figure 1: Map of starting locations for our simulations.

	LABEL	LATITUDE	LONGITUDE	COMMENTS
★	1. WHEAT ALBERTA	31.44N	115.67W	Large wheat production
★	2. WILD CANADA	46.83N	76.11W	Blueberries
★	3. VEGGIES WI	44.07N	90.91W	Vegetable growing area
★	4. FOREST CO	37.51N	107.91W	
★	5. CROPS CA	36.95N	121.54W	Major agricultural area (strawberries)
★	6. TOBACCO NC	35.87N	78.10W	Tobacco production
★	7. CROPS OKLA	33.54N	94.64W	
★	8. BAJA CA	31.43N	115.67W	Coastal area
★	9. WHEAT MEXICO	27.70N	109.01W	Major region of wheat production in Mexico
★	10. GREEN MEXICO	19.63N	99.19W	Site for green revolution, maize and wheat

Figure 2: Details of starting locations.

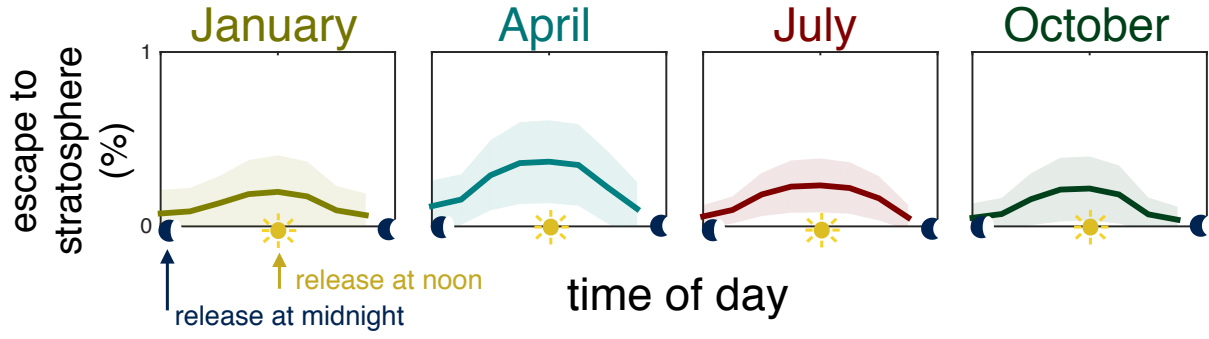


Figure 3: A small fraction of spores escapes into the stratosphere, especially during highly convective conditions typically found during the day. Left to right: average fraction of spores escaping into the stratosphere as a function of time of the day for the 4 months we simulated. Averaged over the 10 starting locations.

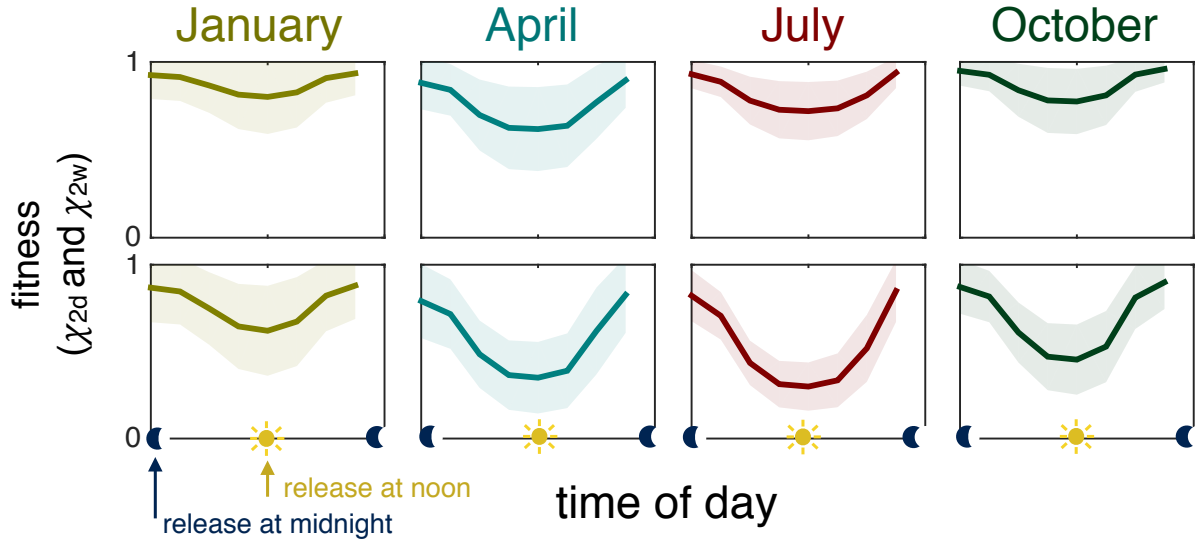


Figure 4: Fitness for longer lived spores follows similar patterns as those described in the main text. Selective pressure is released for longer lived spores that survive flights in most conditions. Top row: fitness for spores with lifetime 2 weeks, Bottom row: fitness for spores with lifetime 2 days.

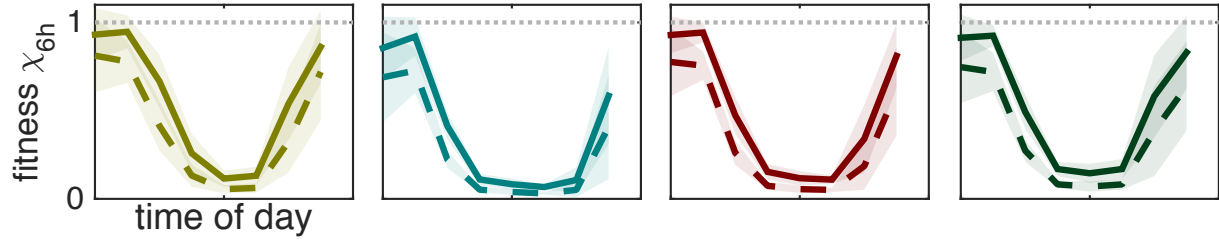


Figure 5: Results vary with settling velocity. From left to right: fitness for spores with lifetime 6 hours for the 4 months simulated as described in the main text. Full simulation described in the main text with settling velocity 6 mm/s (colored dashed lines); with double settling velocity 12 mm/s (colored solid lines); settling velocities of 6 cm/s , 10 times larger than the simulations showed in the main text, causes spores to always sediment in less than 6 hours (dotted gray lines). Patterns in fitness occur even for these large spores, if a shorter lifetime is considered (Data not shown).

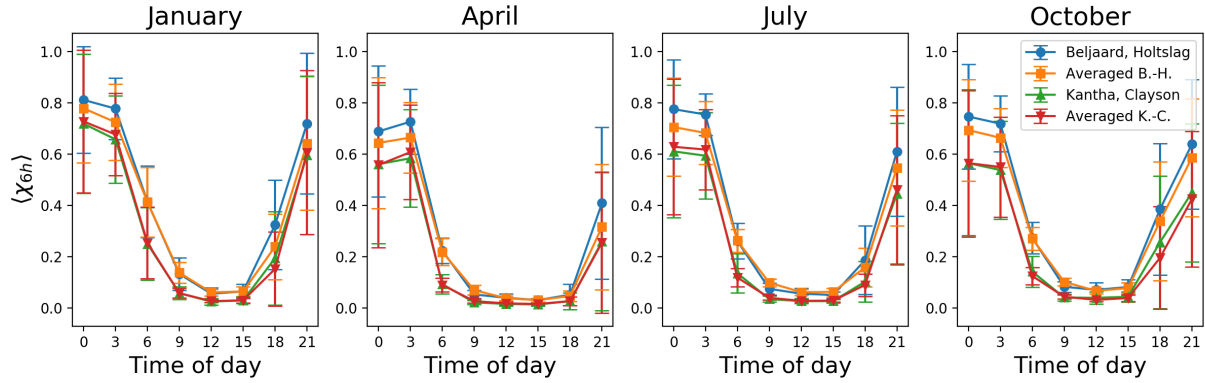


Figure 6: Robustness of results with respect to different closures for modelisation of turbulent fluctuations of vertical wind. Left to right: Fitness of spores with lifetime 6 h , for the months of January, April, July and October. Different colors / symbols correspond to different closure schemes: Beljaars and Holtslag with the z -dependence (blue dots); Beljaars and Holtslag averaged over z (green squares); Khantar and Clayson with the z -dependence (green upward triangles); Khantar and Clayson averaged over z (red downward triangle).

I. LAGRANGIAN SIMULATIONS WITH WEATHER DATA USING HYSPLIT

In this work we simulate atmospheric transport using the Lagrangian approach, i.e. we follow the trajectories of many individual particles rather than describing the evolution of the concentration of particles. We model spores as passive tracers with an additional gravitational settling velocity, which is a commonly used approximation in geophysical transport. Neglecting inertial effects is justified for typical spores (about $10\ \mu m$ in radius and density of water) whose Stokes timescale is about 1 ms, much smaller than the Kolmogorov timescale, the smallest characteristic timescale for turbulent transport, which is $\tau_\eta \sim 0.1$ s. Stokes numbers of the order of 0.01 result in cancellation of many terms in the general Maxey-Rayley form of the equation of motion for spheres immersed in a fluid[4]. Under these assumptions spore trajectories are solutions of the following ordinary differential equation:

$$\frac{d\mathbf{P}(t)}{dt} = \mathbf{V}_{\text{wind}}[\mathbf{P}(t), t] + \mathbf{V}_G, \quad (1)$$

where $\mathbf{P}(t)$ is the position of the particle at time t ; $\mathbf{V}_{\text{wind}}[\mathbf{P}(t), t]$ is the instantaneous velocity of the wind at the location occupied by the particle at time t and \mathbf{V}_G is the gravitational settling. A complete description including all dynamical degrees of freedom of the wind velocity field from the smallest to the largest scales (mm to hundreds of km) is practically inaccessible. To overcome the problem, HYSPLIT takes a widely used approach, and describes the flow from the largest scale down to a certain spatio-temporal resolution, whereas the structure of the velocity field below this intermediate scale is modelled. The large-scale velocity of the wind is provided by regional meteorological models and a stochastic term describes the small-scale turbulence which is in general neither stationary nor homogeneous. Spore trajectories can be computed through a Langevin equation:

$$\frac{d\mathbf{P}(t)}{dt} = \mathbf{V}_{\text{meteo}}[\mathbf{P}(t), t] + \mathbf{V}'[\mathbf{P}(t), t] + \mathbf{V}_G. \quad (2)$$

Here $\mathbf{V}_{\text{meteo}}$, \mathbf{V}' and \mathbf{V}_G are the large-scale wind velocity from meteorological datasets; the turbulent velocity fluctuations and the gravitational settling velocity respectively. Lagrangian simulations described in the maintext are performed using the Hybrid Single Particle Lagrangian Integrated Trajectory (HySPLIT) model [5], an open source code developed at the Air Resource Laboratory of the National Ocean and Atmospheric Administration (ARL-NOAA) in the US.

a. Numerical technique To find a numerical solution of Eq. 2 we consider the following equivalent discrete-time set of equations:

$$\begin{aligned} X(t + \Delta t) &= X_{\text{Adv}}(t + \Delta t) + U'(t + \Delta t)\Delta t G_X \\ Y(t + \Delta t) &= Y_{\text{Adv}}(t + \Delta t) + V'(t + \Delta t)\Delta t G_Y \\ Z(t + \Delta t) &= Z_{\text{Adv}}(t + \Delta t) + W'(t + \Delta t)\Delta t G_Z + V_G\Delta t \end{aligned}$$

where Δt is the time step; $(X, Y, Z) = \mathbf{P}$ are the three components of spore position; the pedices Adv indicates new positions computed after advection by the large-scale wind speed, $(U', V', W') = \mathbf{V}'$ are the turbulent velocity components and G_X, G_Y, G_Z are scaling factors depending on the adopted coordinates. Wind fields for advection are taken from the North American Regional Reanalyses (NARR)[6], which is an extended dataset of meteorological variables on a regular grid covering the whole North American continent. This dataset is the result of a matching procedure between outputs of numerical models and sparse observations of many atmospheric variables. NARR data are given on a Lambert conformal grid with 309 x 237 horizontal points and 24 levels on a vertical pressure-sigma coordinates system. The nominal horizontal resolution is 32 km. Starting from 1979 to today the state of the atmosphere is available at a time resolution of 3 hours. The same system of horizontal coordinates as that of the meteorological dataset is used; fields are interpolated on an internal sigma-terrain-following system in the vertical direction, whose coordinates follow the orography of the terrain. The time marching for advection is made in two steps, initially computing a first guess position:

$$\mathbf{P}'(t + \Delta t) = \mathbf{P}(t) + \mathbf{V}(\mathbf{P}, t)\Delta t,$$

where $\mathbf{V}(\mathbf{P}, t)$ is the resolved wind velocity at time t interpolated at the particle position and then giving a final position

$$\mathbf{P}(t + \Delta t) = \mathbf{P}(t) + \frac{1}{2} [\mathbf{V}(\mathbf{P}, t) + \mathbf{V}(\mathbf{P}', t + \Delta t)] \Delta t.$$

As mentioned before, turbulent velocities are realizations of stochastic processes [7]. For each component such processes are described by the following equations:

$$\begin{aligned} U'(t + \Delta t) &= R(\Delta t)U'(t) + U''\sqrt{1 - R(\Delta t)^2} \\ V'(t + \Delta t) &= R(\Delta t)V'(t) + V''\sqrt{1 - R(\Delta t)^2} \\ \left(\frac{W'}{\sigma_W}\right)(t + \Delta t) &= R(\Delta t)\left(\frac{W'}{\sigma_W}\right)(t) + \\ &+ \left(\frac{W''}{\sigma_W}\right)(t)\sqrt{1 - R(\Delta t)^2} + T_{L_W}(1 - R(\Delta t))\frac{\partial\sigma_3(t)}{\partial z} \end{aligned}$$

with

$$\sigma_W(t + \Delta t) = \sigma_W(t) + W'(t)\Delta t\frac{\partial\sigma_3(t)}{\partial z}$$

and where the autocorrelation function R is

$$R(\Delta t) = e^{-\frac{\Delta t}{T_{L_i}}}$$

with $T_{L_i} = T_{L_W}, T_{L_U}$ or T_{L_V} Lagrangian time scales, assumed as constant in the model and equal to $T_{L_W} = 100s$ and $T_{L_U} = T_{L_V} = 10800s$. The random velocities U'', V'', W'' are computed as

$$U'' = \sigma_1\lambda_1, \quad V'' = \sigma_2\lambda_2, \quad W'' = \sigma_3\lambda_3,$$

where λ_i are realizations of gaussian random processes with mean 0 and unitary standard deviation and the σ_i^2 are the turbulent velocity variances which values are function of both time and space and depend on the turbulent parameterization (turbulence closure) adopted, discussed below.

For the horizontal components of the velocity the problem is closed connecting turbulent velocity variances with the deformation gradient of the large scale wind field:

$$\sigma_{1,2} = \sqrt{\frac{1}{\sqrt{2}T_{L_U}}(c\Delta X)^2 \left[\left(\frac{\partial v}{\partial x} + \frac{\partial u}{\partial y}\right)^2 + \left(\frac{\partial u}{\partial x} - \frac{\partial v}{\partial y}\right)^2 \right]^{\frac{1}{2}}}$$

where $c = 0.14$ and ΔX is the horizontal grid step [1, 2]

Vertical turbulence requires a preliminary evaluation of the atmospheric boundary layer (ABL) stability, which is done by HySPLIT by evaluating the *Monin-Obukhov length* L , that is a dimensional parameter related with the stability of the surface layer, the lower part of the ABL. It is positive or negative when the ABL state is respectively stable or unstable.

The expression for L is

$$L = -\frac{(u^*)^3}{kg \frac{\langle w'\theta' \rangle}{\theta}}.$$

The parameter $u^* = [\langle u'w' \rangle^2 + \langle v'w' \rangle^2]^{\frac{1}{4}} = |\frac{\tau_s}{\rho}|^{\frac{1}{2}}$, called the *friction velocity*, is related with the turbulent stress at the surface τ_s and the air density ρ ; the covariances $\langle u'w' \rangle$ and $\langle v'w' \rangle$ are the kinematic momentum fluxes at the surface. At the denominator g is the gravity acceleration, $k = 0.4$ is the von Karman constant, θ is the potential temperature and $\langle w'\theta' \rangle$ is proportional to the turbulent heat flux at the surface. From a physical point of view, L measures the relative contributions to turbulent kinetic energy given by buoyant production and shear production, representing the height at which these two contributions are equal.

During unstable conditions another velocity scale can be introduced, the convective velocity $W^* = [\frac{gZ_i}{\theta} \langle w'\theta' \rangle]^{\frac{1}{3}}$, where Z_i is the boundary layer depth, that is another important parameter involved in the computation of turbulent motions. All these parameters are internally evaluated by the model from meteorological data (for more details see [5]) and they are involved in the computation of vertical turbulent velocities which are obtained by semi-empirical formulas. Several possible semi-empirical parameterizations, also called closures, can be chosen. A possible choice is to follow Khantar and Clayson equations [8], according to which the vertical velocity variances during stable conditions are given by

$$\begin{aligned} \sigma_3^2 &= 3.0(u^*)^2 & (\text{surface layer}) \\ \sigma_3^2 &= 3.0(u^*)^2 \left(1 - \frac{z}{Z_i}\right)^{\frac{3}{2}} & (\text{rest of the ABL}), \end{aligned}$$

while unstable conditions are modeled as follows:

$$\begin{aligned} \sigma_3^2 &= 1.74(u^*)^2 \left(1 - 3\frac{z}{L}\right)^{\frac{2}{3}} & (\text{surface layer}) \\ \sigma_3^2 &= 3.0(W^*)^2 \left(\frac{z}{Z_i}\right)^{\frac{2}{3}} \left(1 - \frac{z}{Z_i}\right)^{\frac{2}{3}} \times \left(1 + 0.5R^{\frac{2}{3}}\right) & (\text{rest of the ABL}) \end{aligned}$$

where $R = 0.2$.

An alternative approach is given by Beljaars and Holtslag [9], which identifies the diffusion coefficient for particles with the diffusion coefficient for heat, and then converts them into turbulent velocities. According to this idea the vertical diffusion coefficient K_3 is given by the following expression:

$$K_3 = kw_h z \left(1 - \frac{z}{Z_i}\right)^2,$$

where the stability parameter w_h changes according to the stability of the ABL and is a function of friction velocity, Monin-Obukhov length, and convective velocity as described in [3]. Therefore, once diffusion coefficients have been computed, the turbulent velocity variances result from

$$\sigma_3 = \sqrt{\frac{K_3}{T_{Lw}}}.$$

Both parameterizations provide vertical turbulent velocities as a function of the altitude. We consider the further possibility to first compute the vertical profiles of turbulent diffusivities at each x, y location, and then averaging them over the ABL, so that the vertical fluctuation does not depend on height above the ground (a condition that we have labeled “vertically uniform” in Figure 2 of the main paper).

Analogous semiempirical descriptions are used also for the stratosphere, above the ABL, where turbulent velocities quickly become negligible and their contribution is subdominant in the dynamics with respects to the stronger large scale circulation. The main results showed in the main text are obtained using the Beljaars and Holtslag scheme. We have tested the robustness of our results by changing the parameterization of vertical turbulence, and we find that typical patterns of our statistical observables are preserved in all cases (see Figure 6).

A further player in in the dynamics is gravitational sedimentation, described by a constant downward velocity. Approximating spores as spheres with the same volume of the spore, the sedimentation velocity can be computed starting from spore equivalent radius r and its density ρ_S

$$V_G = g\tau_S = \frac{2(\rho_S - \rho_{Air})gr^2}{9\mu}$$

where τ_S is the Stokes time, $\mu = 1.81 \cdot 10^{-5} Pa \cdot s$ is the dynamical viscosity of air, ρ_S and ρ_{Air} are spore and air densities respectively. This is the only parameter of the dynamics that depends on the fungal species, specifically on spore size, shape and density. We set this parameter to $V_G = 6 mm/s$, resulting from characteristic parameters of the wheat pathogen *Puccinia Graminis* that is largely present in the North American continent. Although this is a specific choice, many species have similar sedimentation velocities. Moreover, gravitational settling affects fitness significantly less than vertical turbulence as shown for χ_{6h} in Figure 2 of the main text, and Figure 5.

The last factor affecting residence times is dry deposition to ground which is computed

assuming that the flux $j(\mathbf{x}, t)$ of spores to the ground is proportional to concentration $\theta(\mathbf{x}, t)$ close to the soil:

$$j(\mathbf{x}, t) = V_d \theta(\mathbf{x}, t)|_{z=0}$$

where the parameter V_d has the dimension of a velocity and has been taken equal to the gravitational settling velocity, as appropriate for particles larger than about $1 \mu m$ [10]. Assuming that deposition occurs in a layer of thickness ΔZ_d above the ground level and taking particle concentration as constant within this layer, the time employed by the mass present in ΔZ_d to be completely deposited is equal to $\frac{\Delta Z_d}{V_d}$ and hence the fraction of mass deposited in a time step Δt is given by the ratio $\frac{V_d \Delta t}{\Delta Z_d}$. This mass drop is reproduced removing randomly particles below ΔZ_d with probability

$$P = \frac{V_d \Delta t}{\Delta Z_d}$$

. As pointed out above and showed in Figure 2 of the main text, deposition velocities affect fitness quantitatively, but do not affect the qualitative patterns observed. Wet deposition will affect the results, but only modifies the picture if fungi are able to release spores when rain events are more probable. Although this is a fascinating possibility, and some evidence is starting to emerge in this direction, this remains outside the scope of the present work and will be examined in detail elsewhere.

Table I: Comparison of physical spore parameters for two species.

Species	size [μm]	density [$\frac{g}{cc}$]	Stokes time [s]
<i>Puccinia graminis</i>	28.3 (length)	0.47	$1.78 \cdot 10^{-3}$
	17.5 (width)		
<i>sclerotinia sclerotiorum</i>	12 (length)	0.44	$1.95 \cdot 10^{-4}$
	6 (width)		

-
- [1] Smagorinsky J (1963). General circulation experiments with the primitive equations: 1. The basic experiment. *Mon. Weather Rev.* **91**:99-164.

- [2] Deardorff JW (1973). Three-dimensional numerical modeling of the planetary boundary layer. *In Workshop on Micrometeorology* D.A. Haugen (Ed.), American Meteorological Society, Boston, 271-311
- [3] Draxler RR and Hess GD (2018). Description of the HYSPLIT₄ modeling system, *NOAA Technical Memorandum ERL ARL-224*. [https : //www.arl.noaa.gov/wp_arl/wp-content/uploads/documents/reports/arl-224.pdf](https://www.arl.noaa.gov/wp_arl/wp-content/uploads/documents/reports/arl-224.pdf)
- [4] Maxey MR and Riley JJ (1983). Equation of motion for a small rigid sphere in a nonuniform flow *The Physics of Fluids* **26**:883
- [5] Stein AF, Draxler RR, Rolph GD, Stunder BJB, Cohen MD and Ngan F. NOAA’s HYSPLIT atmospheric transport and dispersion modeling system, *Bull. Amer. Meteor. Soc.* **96**: 2059-2077 (2015)
- [6] Mesinger F, DiMego G, Kalnay E, Mitchell K, and Coauthors. North American Regional Reanalysis. *Bulletin of the American Meteorological Society* **87**: 343–360 (2006)
- [7] Wilson JD, Legg BJ, and Thomson DJ. Calculation of particle trajectories in the presence of a gradient in turbulent velocity variance, *B. Layer Meteorol.* **27**: 163-169 (1983)
- [8] Kantha LH and Clayson CA. *Small Scale Processes in Geophysical Fluid Flows, Vol. 67, International Geophysics Series* Academic Press, San Diego, CA, 883 pp. (2000)
- [9] Beljaar ACM, and Holtslag AAM. Flux parameterizations over land surfaces for atmospheric models. *J. Appl. Meteorol.* **30**: 327-341 (1991)
- [10] *Smoke, Dust and Haze, Fundamentals of Aerosol Dynamics*, SK Friedlander, Oxford University Press, Oxford (2000)